Resonance Sidepath in Muon Catalyzed Fusion

P. Froelich and J. Wallenius
Department of Quantum Chemistry, Box 518, S-751 20 Uppsala, Sweden
(Received 21 April 1995)

We have investigated a previously unconsidered sidepath in muon catalyzed fusion. We have found that high formation rates of metastable $dt\mu^*$ molecules in $t\mu(2s)$-D_2 collisions and their subsequent decay into $t\mu(1s)$ *or* $d\mu(1s)$ atoms open a return path for the muon from tritium to deuterium. This process can be considered as muon transfer from $t\mu(2s)$ to $d\mu(1s)$ via three-body resonances of $dt\mu^*$. This enlarges the $d\mu(1s)$ population and quenches the muon cycling rate, in agreement with experimental findings.

PACS numbers: 36.10.Dr, 25.45.–z

Chemical confinement of nuclei in muonic molecules such as $dt\mu$ leads to rapid nuclear fusion, according to the reaction

$$dt\mu \longrightarrow \alpha + n + \mu + 17.6\ \text{MeV}. \qquad (1)$$

This phenomenon is known as muon catalyzed fusion (μCF) [1,2]. The formation of muonic molecules in D_2-T_2 mixtures is a spontaneous and recurrent process that occurs without any external energy input. Each muon can catalyze 150–200 fusion events, releasing energy 20 times larger than its rest mass. Since the formation of muonic molecules is a multistep collisional process, the efficiency of μCF depends on macroscopic conditions such as temperature, medium density, and its composition, and can be optimized with the help of the kinetic theory based on the microscopic collisional rates and cross sections.

An over 10 year old puzzle of μCF consists of the fact that the experimentally measured muon cycling rate [3] is *smaller* than predicted by theory. In the present paper we present a new model that resolves this discrepancy.

Our theory introduces a previously unconsidered sidepath into the main cycle of μCF, due to the here obtained high formation rates of *metastable states* of $dt\mu$ in $t\mu(2s)$-D_2 collisions. The states under consideration are situated in the dissociative continuum of $dt\mu$ just below the $t\mu(2s) + d$ threshold. If these states are formed during the cascade of the $dt\mu$ cycle, they will either fuse or decay into highly energetic $d\mu(1s)$ or $t\mu(1s)$ atoms. The branching ratio into the fusion channel is expected to be small. Thus the low sticking fraction previously found [4] may not have a significant impact on the μCF cycle, but this issue should be further investigated. The question then arises whether the sidepath branching into the decay channel is sufficiently populated to alter the kinetics of μCF. We will show that this may very well be the case.

A simplified scheme of the μCF cycle is given in Fig. 1. Muons are captured in the highly excited states of muonic atoms and deexcite through various radiative and collisional processes. The process of muon transfer, occurring because of the isotopic energy difference between the atomic states $d\mu(n)$ and $t\mu(n)$, tends to accumulate the muons on tritium in a rather irreversible way.

Prevailing theory foresees that muons reaching the $t\mu(2s)$ level are deexcited to the ground state of tritium, $t\mu(1s)$, where formation of $dt\mu$ bound states takes place. We propose that fast formation of metastable $dt\mu^*$ and its subsequent decay into $t\mu(1s)$ *or* $d\mu(1s)$ opens a *return* path to deuterium. The process can be considered as muon transfer from $t\mu(2s)$ to $d\mu(1s)$. To justify the presence of the sidepath we will show that the formation rate of metastable $dt\mu^*$ is high enough to successfully compete with deexcitation of the $n = 2$ levels of the tritium atom.

Since several of the resonances are located within the dissociation energy of D_2 ($\simeq 4.5$ eV) below the $t\mu(2s)$ threshold, we will here consider the Vesman formation mechanism [5], whereby the excess binding energy is transferred to the rovibrational degrees of freedom of the host D_2 molecule in the process

$$t\mu(2s) + D_2 \longrightarrow [(dt\mu^*)dee]_{\nu K}, \qquad (2)$$

where ν and K are the vibrational and rotational quantum numbers of the resulting hybrid molecule, and D_2 is assumed to be in the ground state with $\nu = 0$, $K_i = 0$.

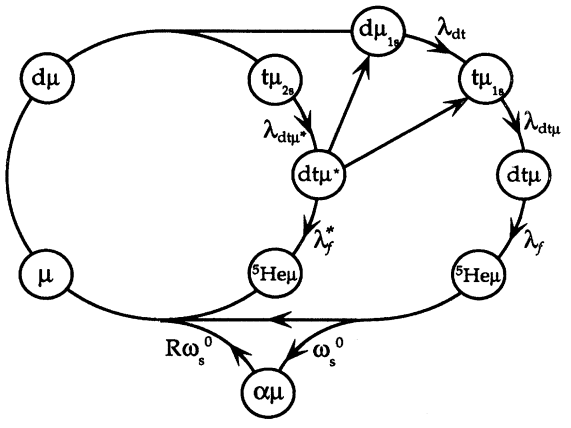

FIG. 1. Simplified scheme of the μCF cycle, including the proposed sidepath.

 0031-9007/95/75(11)/2108(4)$06.00

The cross section for the above reaction is given by the Breit-Wigner relation

$$\sigma = \frac{\pi}{k^2} \frac{\Gamma_{ent}\Gamma_r}{(E_{coll} - E_{res})^2 + \frac{1}{4}(\Gamma_{ent} + \Gamma_r)^2}. \quad (3)$$

The Vesman resonant energy E_{res} satisfies the energy conservation condition

$$E_{res} + E_b = \Delta E_{rovib} + \Delta E_{hf}, \quad (4)$$

where E_b is the binding energy of the metastable molecular state with respect to the $t\mu(2s)$ threshold. ΔE_{rovib} is the difference between the rovibrational levels of the hybrid molecule $[(dt\mu^*)dee]$ and the D_2 molecule, while ΔE_{hf} is the difference in hyperfine splitting of atomic and molecular levels.

Γ_r is the reactive scattering width, given by

$$\Gamma_r = \Gamma_{Aug} + \Gamma_f + \Gamma_c. \quad (5)$$

Here, Γ_{Aug} is the width for Auger decay of the hybrid molecule, Γ_f is the fusion width, and Γ_c is the width for Coulombic decay.

Γ_{ent}^{JK} is the so-called entrance width, here evaluated according to the theory proposed by Lane [6]:

$$\Gamma_{ent} = \frac{4mk}{(4\pi)^2} \sum_{M_J,M_K} \int d\hat{k} |N(\boldsymbol{k}, V_{31}) + N(\boldsymbol{k}, V_{32})|^2, \quad (6)$$

with

$$N(\boldsymbol{k}, V_{ij}) \equiv \langle e^{i\boldsymbol{k}\cdot(\boldsymbol{r}_3 - \boldsymbol{R}_{12})} \Psi_{0K_i}(\boldsymbol{r}_{12}) | V_{ij} | \times \bar{\Phi}_{\nu K}(\boldsymbol{R}_{31} - \boldsymbol{r}_2) \chi_\nu(r_{31}) Y_{JM_J}(\hat{r}_{31}) \rangle. \quad (7)$$

In the above expression, the final wave function of the entire system is written in a product approximation. In the initial channel, Ψ_{00} is a wave function describing the nuclear motion of D_2 in the electronic Born-Oppenheimer (BO) potential, and the relative motion of D_2 with respect to $t\mu$ is described by a plane wave of momentum k. In the reaction channel, $\bar{\Psi}_{\nu K}$ is a BO wave function describing the motion of d with respect to $dt\mu$ treated as a point charge, and χ_ν is the pseudo wave function obtained from the complete three-body wave function of quasibound $dt\mu^*$ of J symmetry by integrating out the muon coordinate. V_{ij} denotes the interparticle interaction, and m is the reduced mass for fragments in the initial channel. Coordinate labeling is explained in Fig. 2.

It is convenient to express the other coordinates in terms of $\boldsymbol{r}_{31}$ and $\boldsymbol{R} \equiv \boldsymbol{R}_{31} - \boldsymbol{r}_2$. We then have

$$e^{i\boldsymbol{k}\cdot(\boldsymbol{r}_3 - \boldsymbol{R}_{12})} \Psi_{00}(\boldsymbol{r}_{12}) \equiv e^{i\boldsymbol{k}\cdot(f\boldsymbol{r}_{31} + g\boldsymbol{R})} \Psi_{00}(\boldsymbol{R} - h\boldsymbol{r}_{31}), \quad (8)$$

where f, g, and h are kinematical mass factors specified in Ref. [6]. As the wave functions χ_ν describe a localized system, *and* the interaction V_{31} is of short range, we may assume that the range of $\boldsymbol{r}_{31}$ integration, determined by the factor $V_{31}\chi_\nu(r_{31})$, is much less than the range of $\boldsymbol{R}$. Then an approximation to (8) comes from the first terms of the Taylor expansion of the initial D_2 wave function,

$$\Psi_{00}(\boldsymbol{R} - h\boldsymbol{r}_{31}) \simeq \Psi_{00}(\boldsymbol{R}) - h\boldsymbol{r}_{31} \cdot \nabla\Psi_{00}(\boldsymbol{R}). \quad (9)$$

The entrance width $\Gamma_{ent}^{JK}(k)$ is evaluated by keeping the two first terms of the partial wave expansion of the plane wave in (8), i.e., considering s-wave and p-wave formation, neglecting the contribution from the spectator deuteron $N(\boldsymbol{k}, V_{32})$, integrating over angles $\hat{r}$, $\hat{R}$, and $\hat{k}$, and taking the sum over magnetic numbers M_J and M_K (details will be published elsewhere). Four combinations of final angular momenta appear:

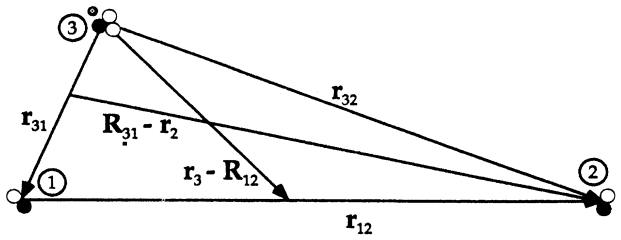

FIG. 2. Coordinates of the $\langle t\mu\text{-}D_2 \rangle$ system. $d = 1, 2$, $t\mu = 3$, $\boldsymbol{r}_{ij} = \boldsymbol{r}_i - \boldsymbol{r}_j$. $\boldsymbol{R}_{ij}$ denotes center of mass coordinate.

$$\frac{\Gamma_{ent}^{00}}{4mk} = (T^{\mu_1}T^{e_1})^2 + \frac{2h}{3} T^{\mu_1}T^{e_1}T^{\mu_2}T^{e_2} + \frac{7}{15} \times (hT^{\mu_2}T^{e_2})^2,$$

$$\frac{\Gamma_{ent}^{01}}{4mk} = 3(T^{\mu_1}T^{e_1})^2 - \frac{2h}{3} T^{\mu_1}T^{e_1}T^{\mu_2}T^{e_2} + \frac{1}{3} \times (hT^{\mu_2}T^{e_2})^2,$$

$$\frac{\Gamma_{ent}^{10}}{4mk} = 3(T^{\mu_1}T^{e_1})^2 - \frac{2h}{3} T^{\mu_1}T^{e_1}T^{\mu_2}T^{e_2} + \frac{1}{3} \times (hT^{\mu_2}T^{e_2})^2,$$

$$\frac{\Gamma_{ent}^{11}}{4mk} = \frac{96}{5}(T^{\mu_1}T^{e_1})^2 + \frac{2h}{3} T^{\mu_1}T^{e_1}T^{\mu_2}T^{e_2} + \frac{1}{3} \times (hT^{\mu_2}T^{e_2})^2,$$

where the radial matrix elements T are given by

$$T_\nu^{\mu_1} = \langle j_J(fkr) | E_{J\nu}^b | \chi_\nu(r) \rangle,$$

$$T_\nu^{\mu_2} = \langle j_{J'}(fkr) r | E_{J\nu}^b | \chi_\nu(r) \rangle,$$

$$T_\nu^{e_1} = \langle \psi_0(R) | j_K(gkR) | \bar{\psi}_\nu(R) \rangle,$$

$$T_\nu^{e_2} = \left\langle \frac{\partial \psi_0}{\partial R} | j_{K'}(gkR) | \bar{\psi}_\nu(R) \right\rangle, \quad (10)$$

with $J' = |J - 1|$, $K' = |K - 1|$, and $E_{J\nu}^b$ being the binding energies specified in Table I.

To calculate the matrix elements T^{μ_i}, the wave functions $\chi_\nu(r_{31})$ were obtained variationally using the coupled rearrangement channel method [7], in conjunction with the stabilization technique [4]. The complete three-body wave function $\Phi_{JM}(\boldsymbol{r}, \boldsymbol{R})$ was expanded in terms of 3000 Gaussian basis functions spanned over the three rearrangement channels. The electronic matrix elements T^{e_i} were calculated in the BO approximation, solving the one-dimensional Schrödinger equation using the potential calculated by Kolos, Szalewicz, and Monkhorst [8].

The calculation of the entrance width Γ_{ent}^{JK} is exemplified for the formation of the ninth vibrational state of the $dt\mu^*$ molecule ($\nu = 8$) for which R_{dt} does not exceed

TABLE I. Energies of $dt\mu^*$ ($J = 1$) resonances within the Vesman formation range below the $t\mu(2s)$ threshold, given in eV. First column: pure Coulombic interaction, second column: vacuum polarization potential included in the three-body Hamiltonian. The matrix elements T^{μ} are given in atomic units.

v	E_b^{Coul}	E_b^{vac}	T^{μ_1} $(k \to 0)$	T^{μ_2} $(k \to 0)$
6	−3.187	−3.068	0.0156	0.0071
7	−1.514	−1.397	0.0099	0.0062
8	−0.713	−0.601	0.0105	0.0085
9	−0.324	−0.219	0.0055	0.0062

0.6 a.u. Condition (4) then gives that formation of $dt\mu^*$ with $J = 0$ must be accompanied by the $v = 3$ transition, while formation of the $J = 1$ resonance is possible for $v = 2$. The matrix elements $T_v^{e_i}$ and $T_v^{\mu_i}$ in the limit $k \to 0$ are displayed in Tables I and II, from where also the relevant values of E_{res} can be extracted. The resulting entrance widths Γ_{ent}^{JK} are exemplified in Fig. 3. Note that formation of $J = 0$ states is non-negligible.

It is expected that the main contribution to Γ_r comes from the Auger decay

$$[(dt\mu^*)_{vJ}dee] \to [(dt\mu^*)_{v'J'}de]^+ + e^-. \tag{11}$$

Γ_{Aug} can be found from Fermi's golden rule

$$\Gamma_{Aug} = 2\pi\rho(E)\sum_f |\langle f|H_I|i\rangle|^2, \tag{12}$$

where $|f\rangle$ and $|i\rangle$ are the final and initial states of the system and $\rho(E)$ is the density of final states for a given energy. The interaction operator H_I can be approximated by $H_I = -(\boldsymbol{r_e}\cdot\boldsymbol{d})r_e^{-3}$ where $\boldsymbol{d}$ is the dipole moment operator. We make the following estimation of Γ_{Aug}:

$$\Gamma_{Aug}^{res} \simeq \frac{|\langle\chi_f(r_{dt})\,|r_{dt}|\,\chi_i(r_{dt})\rangle|^2}{|\langle\chi_{01}(r_{dt})\,|r_{dt}|\,\chi_{11}(r_{dt})\rangle|^2}\,\frac{k_{bound}}{k_{res}}\,\Gamma_{Aug}^{11\to01}, \tag{13}$$

where $\Gamma_{Aug}^{11\to01} = 1\times10^{12}\ \mathrm{s}^{-1}$ is the dominant Auger transition rate from the bound $(J,v) = (1,1)$ state. The wave number of the ejected electron is $k = \sqrt{2(E_b - E_I)}$ and χ_f corresponds to the $(J,v) = (0,4)$ state, whose binding energy $E_b = 17.341$ eV matches most closely the ionization energy E_I of the hybrid molecule.

We find that the squared ratio of dipole moments $\simeq 2.6$ and that $k_{bound}/k_{res} = 3.8$, giving $\Gamma_{Aug}^{res} \simeq 1\times10^{13}\ \mathrm{s}^{-1}$. Hence $\Gamma_{Aug} \ll \Gamma_{ent}$. Therefore the exact value of Γ_{ent} becomes irrelevant and the cross section (3) simplifies into

$$\sigma(E_{coll}) = \frac{2\pi^2}{k^2}\,\Gamma_{Aug}\,\delta(E_{coll} - E_{res}). \tag{14}$$

The formation rate as a function of temperature is

$$\lambda_{dt\mu^*} = \rho\,v(E_{res})P(E_{res},T)\sigma(E_{res}), \tag{15}$$

where $P(E_{res},T)$ is the distribution of collision energies at temperature T. Assuming full thermalization, we obtain $\lambda_{dt\mu^*}(T)$ as presented in Fig. 4 for a range of E_{res} stemming from the uncertainty of E_b with respect to remaining relativistic corrections. The temperature dependence derives only from $P(E_{res},T)$, which in reality may be quite different from the Maxwell distribution.

To evaluate the influence of the sidepath on the kinetics of μCF we need to investigate the population dynamics of the $n = 2$ level. $\lambda_{dt\mu^*}$ must be related to all other rates populating and depopulating this level. The inflow of muons arises from radiative and Auger deexcitations from higher levels of $t\mu$, and transfer from $d\mu(n = 2)$, yielding the *arrival* population defined as

$$P_{2s}^{arr}(\tau) = \int_0^\tau \frac{1}{4}\,\lambda_{dt}P_{n=2}^{d\mu}(t) + \sum_{n\geq3}\lambda_{np\to2s}P_{np}(t)\,dt\,, \tag{16}$$

where λ_{dt} is the muon transfer rate and $\lambda_{np\to2s}$ are the relevant radiative and Auger rates. P_{2s}^{arr} is a monotonically growing function of density reaching a saturation value of 16% at liquid hydrogen densities (LHD) [9,10].

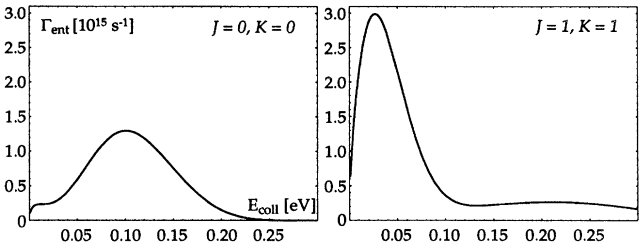

FIG. 3. Γ_{ent}^{JK} (10^{15} s^{-1}) as a function of collision energy.

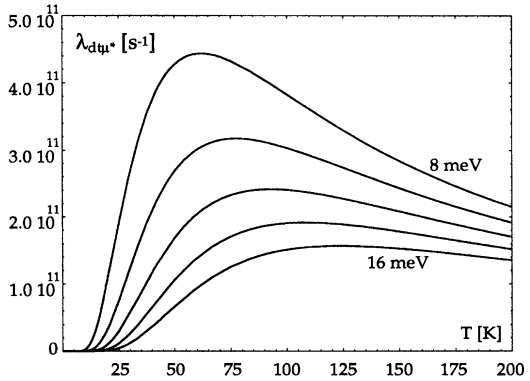

FIG. 4. $\lambda_{dt\mu^*}(T)$ for $\rho = 4.25\times10^{28}\ \mathrm{m}^{-3}$. The different curves give $\lambda_{dt\mu^*}$ for E_{res} in the range 8–16 meV.

TABLE II. Vibrational energies $\bar{E}_{v1}$ (eV) of the hybrid molecule $[(dt\mu)dee]$ assuming a pointlike $dt\mu$, giving transition energies $\Delta E_{rovib}^{v1} = \bar{E}_{v1} - E_{00}$ with respect to the ground state of D_2, with $E_{00} = -4.556$ eV.

v	$\bar{E}_{v1}$	ΔE_{rovib}^{v1}	T^{e_2} $(k \to 0)$	T^{e_1} $(k \to 0)$
0	−4.5825	−0.0265	0.041	0.998
1	−4.2709	0.2851	3.501	0.023
2	−3.9698	0.5862	0.527	0.059
3	−3.6787	0.8773	0.472	0.015

The outflow of muons is due to radiative deexcitation and the formation of $dt\mu^*$ itself. In addition, Stark mixing between the $2s$ and $2p$ levels has to be taken into account. For collision energies exceeding the energy gap caused by vacuum polarization ($\Delta E_{2s\text{-}2p} = 0.236$ eV) conventional collisional Stark mixing dominates, leading to $2s \rightleftharpoons 2p$ transitions with rate $\lambda^{St}_{2p\to 2s} = 1/3\lambda^{St}_{2s\to 2p} \simeq 10^{13}\ \mathrm{s}^{-1}$. For collision energies smaller than $\Delta E_{2s\text{-}2p}$ Stark transitions between the $2s$ and $2p$ states will be inhibited. The Stark mediated $2s \to 2p \to 1s$ deexcitation may still occur during a collision, although with a smaller rate $\lambda_{2s\to 2p\to 1s} \simeq 10^9\ \mathrm{s}^{-1}$ characteristic for a second-order process [9].

Including the processes discussed above, the time evolution of the $t\mu(2s)$ population is given by

$$\frac{\partial P_{2s}}{\partial t} = -(\lambda_{dt\mu^*} + \lambda_{2s\to 2p\to 1s} + \lambda^{St}_{2s\to 2p})P_{2s}(t) + \lambda^{St}_{2p\to 2s}P_{2p}(t) + \frac{1}{4}\lambda_{dt}P^{d\mu}_{n=2}(t) + \sum_{n\geq 3}\lambda_{np\to 2s}P_{np}(t)\,. \quad (17)$$

We can now introduce the arrival population $P^{arr}_{dt\mu^*}$ by its relation to the population P_{2s},

$$P^{arr}_{dt\mu^*}(\tau) = \int_0^\tau \lambda_{dt\mu^*}P_{2s}(t)\,dt\,. \quad (18)$$

Equations (17) and (18) were solved numerically by a finite difference method, taking $\lambda_{dt\mu^*} = 1 \times 10^{11}\ \mathrm{s}^{-1}$.

At small collision energies, both Stark mixing and the Stark mediated $2s \to 2p \to 1s$ deexcitation are slower than molecular formation. Therefore, the formation process drains almost all muons arriving to the $2s$ state, and one has $P^{arr}_{dt\mu^*} \simeq P^{arr}_{2s}$, which approaches 16% at LHD. This case is physically relevant assuming fast thermalization at the $n = 2$ level, and is depicted in Fig. 5(a).

We are now able to discuss the population of $d\mu(1s)$ atoms. It is to be emphasized that the return path model invalidates the traditional definition of q_{1s} being the probability of a $d\mu$ atom formed in a highly excited state arriving in the $d\mu$ ground state, considering one-sided transfer to t. The Coulombic decay of the $dt\mu^*$ resonances opens a return path for the muon from $t\mu(2s)$ to $d\mu(1s)$. If 50% of the $dt\mu^*$ arrival population [Fig. 5(a)] is assumed to end up in the $d\mu(1s)$ state, then its population is raised by $\simeq$0.08 as compared with the predictions of standard theory. Dividing $P^{d\mu}_{1s}$ by C_d we obtain the entity shown in Fig. 5(c), to be compared with the q_{1s} following from the standard model, Fig. 5(b). Recalculation of the muon cycling rate with our values of the $P^{d\mu}_{1s}$ population gives the result presented in Fig. 5(d). If the asymmetric decay of $dt\mu^*$ predicted by Kino and Kamimura [11] is assumed, the agreement with measurements [12] is within error bars.

We conclude that the sidepath model, here presented, alters the kinetics of μCF significantly, enlarging the q_{1s} fraction and lowering the muon cycling rate to values

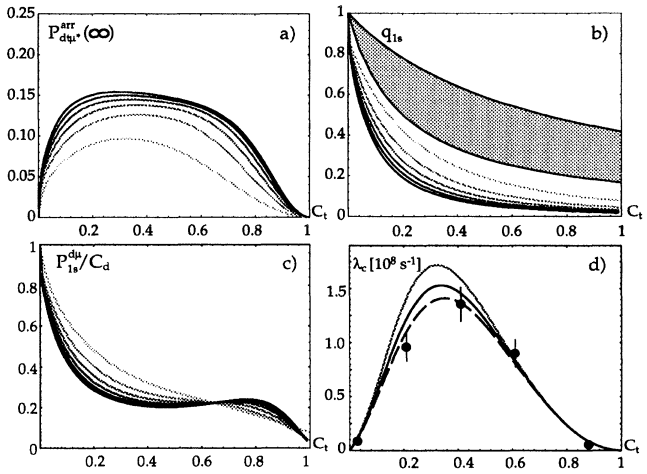

FIG. 5. (a) $P^{arr}_{dt\mu^*}$ with different curves calculated for ρ in the interval (0.2–1.2) × LHD, darker shade corresponding to higher density; (b) q_{1s} fraction, curves—standard theory, shaded region—experiment; (c) $P^{d\mu}_{1s}/C_d$ calculated for symmetric decay of $dt\mu^*$. (d) The *actual* cycling rate λ_c calculated at $\rho = 1.2 \times$ LHD. Solid line—symmetric decay, dashed—asymmetric, gray line—standard theory, and bars—experimental values.

that agree better with measurements. A paradigm shift concerning the q_{1s} fraction comes into view, implying that P_{1s} is the relevant entity. The new understanding of the μCF cycle may be utilized for optimization of experimental conditions to maximize the fusion yield of μCF. The results presented are of importance for muon science in general, and especially for electroweak physics, since the experiments in this area are also concerned with the population of the $2s$ excited muonic atoms.

The authors gratefully acknowledge financial support from the Swedish Natural Science Research Council and the Japanese-German Foundation.

[1] P. Froelich, Adv. Phys. **41**, 405 (1992).
[2] W. H. Breunlich, P. Kammel, J. S. Cohen, and M. Leon, Annu. Rev. Nucl. Part. Sci. **39**, 311 (1989).
[3] A. N. Anderson, in *Muon-Catalyzed Fusion,* edited by Steven E. Jones, Hohann Rafelski, and Hendrik J. Morikhorst, AIP Conf. Proc. No. 181 (AIP, New York, 1988), p. 57.
[4] P. Froelich and A. Flores, Phys. Rev. Lett. **70**, 1595 (1993).
[5] E. Vesman, Sov. Phys. JETP Lett. **5**, 91 (1967).
[6] A. M. Lane, J. Phys. B **21**, 2159 (1988).
[7] M. Kamimura, Phys. Rev. A **38**, 621 (1988).
[8] W. Kolos, K. Szalewicz, and H. Monkhorst, J. Chem. Phys. **84**, 3276 (1986).
[9] V. E. Markushin, Sov. Phys. JETP **53**, 16 (1981).
[10] E. Borie and M. Leon, Phys. Rev. A **21**, 1460 (1980).
[11] Y. Kino and M. Kamimura, in Proceedings of the International Symposium on Muon Catalyzed Fusion, Dubna, 1995 [Hyperfine Interactions (to be published)].
[12] P. Ackerbauer *et al.,* Hyperfine Interact. **82**, 357 (1993).